I043

Flow Properties in Saturated Soils from Differing Behaviour of Dispersive Seismic Velocity and Attenuation

R. Ghose* (Delft University of Technology) & A. Zhubayev (Delft University of Technology)

SUMMARY

A careful look into the pertinent models of poroelasticity reveals that in water-saturated sediments or soils, the seismic (P and S wave) velocity dispersion and attenuation in the low field-seismic frequency band (20-200 Hz) have a contrasting behaviour in the porosity-permeability domain.Taking advantage of this nearly orthogonal behaviour, a new approach has been proposed, which leads to unique estimates of both porosity and permeability simultaneously. Through realistic numerical tests, the effect of maximum frequency content in data and the integration of P and S waves on the accuracy and robustness of the estimates are demonstrated.

Introduction

Previous attempts to use seismic wave dispersion for estimating porosity (n) or permeability (k) have generally considered hard materials or rocks and frequencies in kHz to tens of kHz range. Near-surface seismic data acquired in soft sediments or soils do not have such high frequencies. For water-saturated unconsolidated sediments, Stoll's adaptations of the Biot's theory (Stoll and Bryan, 1970; Stoll, 1977) have earlier been tested on field seismic data (Holland and Brunson, 1988). These models have been found to be capable of predicting the field-observed seismic dispersion for a variety of soil types. In this paper, we shall illustrate our findings on the contrasting behaviour of the dispersive seismic velocity and attenuation in the n-k domain, using the Stoll and Bryan (1970) model. The effects of using only S wave and both P and S waves and the maximum frequency content in the data have been examined for different soil types (gravel, medium sand, fine sand, sandy clay) through numerical tests using realistic material parameters.

Dispersive seismic velocity and attenuation in water-saturated soils

Figures 1(a) and 1(c) illustrate, respectively, the dispersive velocity and attenuation (inverse quality factor) for P wave in water-saturated soft soil, estimated using Stoll and Bryan (1970) model. The dispersion curves for 4 different porosity and permeability values (n=0.35, k=1.09×10^{-9} m^2; n=0.4, k=1.05×10^{-10} m^2; n=0.45, k=1.42×10^{-11} m^2; and n=0.55, k=3.31×10^{-12} m^2) are shown. These values generally correspond to gravel, medium sand, fine sand and sandy clay, respectively. As in Holland and Brunson (1988), we have used Kozeny-Carman relationship to obtain realistic values of k from n:

$$k = \frac{1}{KS_0^2}\frac{n^3}{(1-n)^2}, \qquad (1)$$

where K is an empirical constant and equal to 5 for spherical grains. S_0 can be defined analytically for a sphere as S_0=6/d, where d is the grain diameter. Following Berryman (1981) and Hovem and Ingram (1979), respectively, the tortuosity (γ) and the pore size parameter (a) are obtained as:

$$\gamma = 1 - r\left(1 - \frac{1}{n}\right), \qquad (2)$$

and

$$a = \frac{nd}{3(1-n)}, \qquad (3)$$

where r=0.5 for spheres, and lies between 0 and 1 for other family of ellipsoidal surfaces.

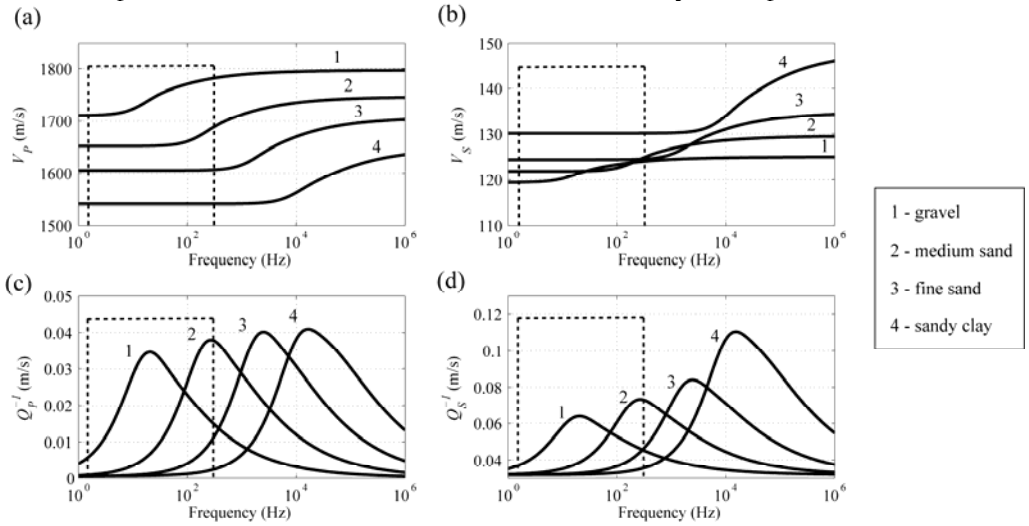

Figure 1 *P and S wave dispersive velocity and attenuation (inverse quality factor) estimated using the Stoll and Bryan (1970) model for 4 different permeability (k) and porosity (n) values, representing 4 different soil types. The dashed box represents the typical field seismic frequency band in soft soil.*

Figures 1(b) and 1(d) show the dispersive velocity and attenuation for S wave for these 4 sets of n and k values. The dashed box in Figure 1 indicates the typical field seismic frequency band for soft soils. Note that for gravel and medium sand (k~10^{-9} m^2 and k~10^{-10} m^2), the velocity dispersion is discernible even in the low field-seismic frequency band. The attenuation is, however, sensitive to

even finer grain soils, as we recognize in the field-frequency band changes in the inverse quality factor (Q_P^{-1} and Q_S^{-1}) even for $k \sim 10^{-11}$ m^2. In other words, at field seismic frequencies, seismic attenuation is sensitive to permeability variation over a wider range than seismic velocity. This effect of the maximum frequency content in data on the permeability sensitivity will have an important bearing on the results to be discussed next.

We calculate the changes - separately for velocity and attenuation over the entire frequency (f) range of interest - when n and k both vary, and all other parameters in the model are assigned fixed realistic values. The individual cost functions for velocity and attenuation (C_i^V and C_i^α, respectively) are defined as follows (Zhubayev and Ghose, 2012):

$$C_i^V = \left(\frac{\sum_f \left| \Delta_i^V \right|^\beta}{\left(\sum_f \left| \Delta_i^V \sigma_i^V(f) \right|^\beta \right)_{\max}} \right)^\beta, \quad (4) \qquad \text{and} \qquad C_i^\alpha = \left(\frac{\sum_f \left| \Delta_i^\alpha \right|^\beta}{\left(\sum_f \left| \Delta_i^\alpha \sigma_i^\alpha(f) \right|^\beta \right)_{\max}} \right)^\beta, \quad (5)$$

where $\Delta_i^V = V_i(f,n,k) - \hat{V}_i(f)$, $V_i(f,n,k)$ being the velocity estimated from the Stoll and Bryan (1970) model and $\hat{V}_i(f)$ representing the field observed velocity dispersion, with i indicating the different wavetypes (P or S). The notations are similar for attenuation α, shown in Eq. (5). The attenuation coefficient α_i is related to Q_i as $\alpha_i = 8.686 \frac{\pi f}{Q_i V_i}$ dB/m. $\sigma_i^V(f)$ and $\alpha_i^V(f)$ denote standard deviation normalized to the mean value. The denominators in Eqs. (4) and (5) compensate for the differences in sensitivity and noise or fluctuation in velocity and attenuation data. We have used β=2 (L_2-norm) for noise-free data. Figures 2(a) and 2(b) show, respectively, the cost functions for P-wave velocity and attenuation for a whole range of n and k. Figures 2(c) and 2(d) illustrate the same for S-wave. For this numerical study, field seismic frequency band (20 - 200 Hz) is considered. Here, the dispersion curves representing the observation, obtained also from Stoll and Bryan (1970), correspond to n=0.4 and k=5×10^{-11} m^2, which are realistic values for fine-grained alluvial sand. The deep blue indicates the cost function minimum.

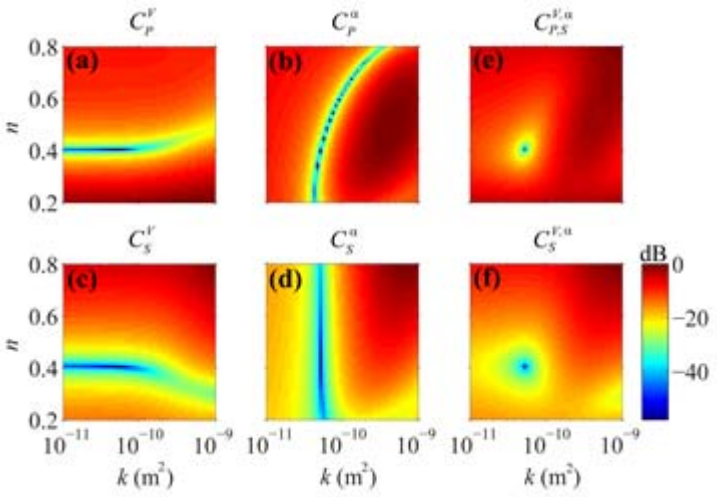

Figure 2 *Cost functions in the n-k domain (see Eq. (4) to Eq. (6)) for: (a) V_P, (b) α_P, (c) V_S, (d) α_S, (e) integrated $V_P+\alpha_P+V_S+\alpha_S$, and (f) integrated $V_S+\alpha_S$. The frequency band used in 20-200 Hz. The deep blue colour indicates the cost function minimum. The difference in behaviour between V_P and α_P and that between V_S and α_S in the n-k domain are driven by the underlying physics of poroelasticity pertinent to such media.*

Remarkably, one can notice in Figures 2(a) and 2(b) that the orientation of the cost function minima line is sharply different between dispersive velocity and attenuation for P waves. The same also holds for S waves (Figure 2(c) and 2(d)). While for velocity, the cost function minima line is nearly parallel to the k-axis, this line is generally parallel to the n axis for attenuation. This shows that while dispersive velocity of seismic waves is more sensitive to n and excepting at very high k is nearly insensitive to k, frequency-dependent seismic attenuation is primarily sensitive to k, and n-sensitivity is relatively insignificant. The cost functions (C_P^V and C_P^α) for P wave shows a sharper minimum in the n-k domain than the cost functions for S wave.

Because the behaviours of dispersive velocity and attenuation are nearly perpendicular to each other in the *n-k* domain, their integration is expected to result in a sharp convergence into a global minimum. We have defined an integrated cost function as follows:

$$C_{P,S}^{V,\alpha} = \left(\frac{\sum_f \left|\Delta_i^V\right|^\beta}{N\left(\sum_f \left|\Delta_i^V \sigma_i^V(f)\right|^\beta\right)_{\max}} + \frac{\sum_f \left|\Delta_i^\alpha\right|^\beta}{N\left(\sum_f \left|\Delta_i^\alpha \sigma_i^\alpha(f)\right|^\beta\right)_{\max}} \right)^\beta, \qquad (6)$$

where $C_{P,S}^{V,\alpha}$ is the integrated cost function for P and S wave velocity and attenuation. N is the number of attributes (i.e., V_P, α_P, V_S, α_S) to be integrated. Figure 2(e) shows the cost function in the *n-k* domain when V_P, α_P, V_S, and α_S are all integrated. Because of the much higher velocity of P wave compared to S wave in water-saturated soil, measuring P-wave dispersion in the field is more challenging than S-wave dispersion. We have, therefore, investigated also the cost function in the *n*-k domain when only V_S and α_S are integrated. The result is shown in Figure 2(f). The global minimum is sharper when both P- and S-wave data are used. However, with only V_S and α_S, the convergence is still very sharp. Unique and correct estimates of both *n* and k (n=0.4, k=5×10^{-11}m^2) are obtained.

We have looked into the effect of the maximum frequency content on the nature of the integrated cost function minima in the *n-k* domain. The result is illustrated in Figure 3. The 4 rows in Figure 3 corresponds to 4 sets of values for *n* and *k*. Figures 3(a) shows the velocity and attenuation integrated cost function for S wave. Figures 3(b) shows the same when both P and S waves are used. The 3 columns in Figure 3(a) represent 3 maximum frequency values in S-wave dispersion data: 80 Hz, 140 Hz and 200 Hz. The 3 columns in Figure 3(b) correspond to 3 maximum frequencies in P-wave data: 100 Hz, 200 Hz and 300 Hz, while S-wave maximum frequency is constant at 80 Hz. The minimum frequency is 20 Hz for all. These frequency limits are realistic for field data acquired in soft soil with conventional seismic sources.

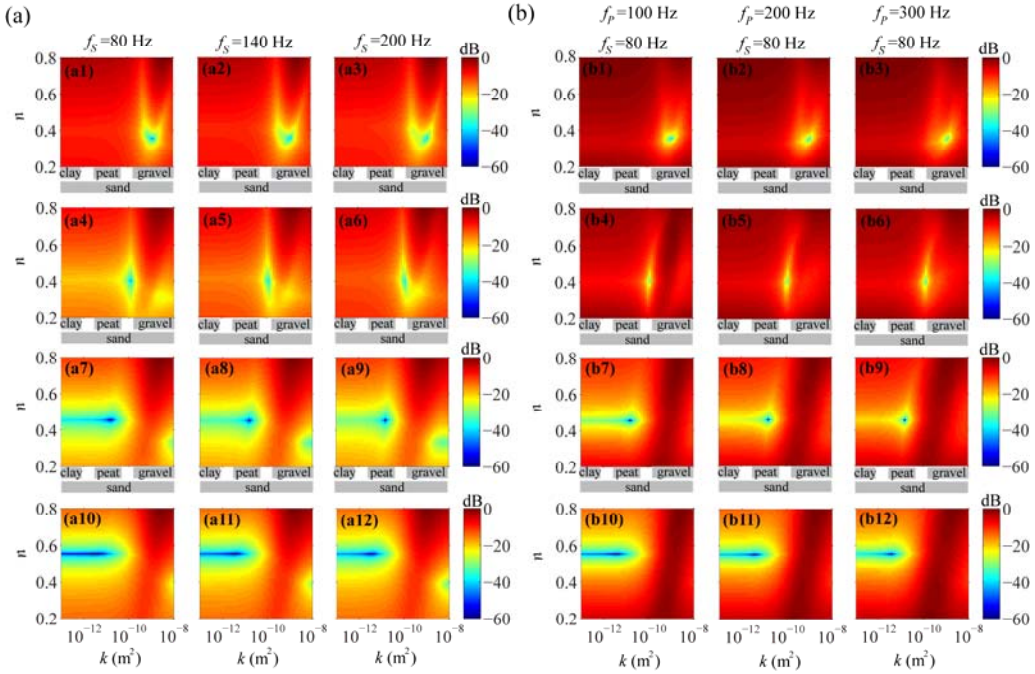

Figure 3 *Effect of the maximum frequency content in the field-observed seismic dispersion on the n and k estimates when (a) V_S and α_S are integrated, and (b) when V_P, α_P, V_S and α_S are integrated, following Eq. (6). The 3 columns represent 3 different values of the maximum frequency in the data. The 4 rows represent 4 different values of n and k (taken as true values).*

It is clear from these numerical tests that *n* can be estimated accurately in all cases. However, estimating correctly the value of *k* depends strongly on the maximum frequency available in the data,

because the *k* variation is sensed by the higher frequencies, especially attenuation (Figure 1). For high *k* (~10^{-9} m^2), typical in coarse-grained sands and gravels, the integration of dispersive velocity and attenuation of S wave with only 80 Hz maximum frequency provides a clear global minimum (Figure 3(a1)). As the maximum frequency limit for S wave increases to 140 Hz and 200 Hz (Figures 3(a2) and 3(a3)) or when P-wave is supplemented to S-wave (Figure 3(b1)-3(b3)), the convergence becomes much sharper. However, when *k* is low (~10^{-10}-10^{-11} m^2, typically representing medium to fine grained sand and peat), having higher frequencies in the data or additional P wave data becomes increasingly advantageous. For instance, for a very low *k* (~10^{-11} m^2), the 20-80 Hz frequency band of S-wave is no longer sufficient to provide a sharp global minimum, and hence one cannot estimate *k* accurately (Figure 3(a7)). However, for this low *k*, if the S-wave frequency band is extended slightly to 20-140 Hz, then the global minimum becomes quite sharp. The global minimum is unambiguous in the results of inversion. Note that even for a very low value for *k* (~10^{-12} m^2, typical for sandy clay and very fine sand) a maximum frequency of 200 Hz in the S-wave data or supplementing P data with low-frequency S data (see Figure 3(a12) and 3(b12)) leads to a sharp global minimum.

We find that this integrated cost function minimization approach, taking advantage of the contrasting behaviour between dispersive velocity and attenuation, is robust. In the illustrations presented in Figures 2 and 3 we have considered noise-free data (hence, $\sigma_i^V(f)$ and $\sigma_i^\alpha(f)$ equal to 1 in Eqs. (4) to (6)). However, we have verified that the presence of ±10% random noise in the velocity dispersion data and ±100% random noise in attenuation data leads to 2% error in *n* and 20% error in *k*. The use of standard deviation normalized to the mean value in the data ($\sigma_i^V(f)$ and $\sigma_i^\alpha(f)$ in Eqs. (4) to (6)) helps significantly in minimizing the effect of random noise in the observed dispersion curves. All parameters in the model other than *n* and *k* have been assigned realistic constant values; if reasonable uncertainties are allowed to those parameters then the errors in the estimated *n* and *k* are still small and they do not exceed the above-mentioned effect of model uncertainty.

Conclusions

A careful look into the pertinent models of poroelasticity reveals that in water-saturated sediments or soils, the seismic (P and S wave) velocity dispersion and attenuation in the low field-seismic frequency band (20-200 Hz) have a contrasting behaviour in the porosity-permeability domain. Taking advantage of this nearly orthogonal behaviour, a new approach has been proposed, which leads to unique estimates of both porosity and permeability simultaneously. Through realistic numerical tests, the effect of maximum frequency content in data and the integration of P and S waves on the accuracy and robustness of the estimates are demonstrated.

Acknowledgements

This research is supported by Deltares and Delft Earth research programme of Delft University of Technology.

References

[1] Berryman, J.G. (1981). "Elastic wave propagation in fluid-saturated porous media", J. Acoust. Soc. Am. 69, 416-424.

[2] Holland, C.W., and Brunson, B.A. (1988). "The Biot-Stoll sediment model: an experimental assessment", J. Acoust. Soc. Am. 84, 1437-1443.

[3] Hovem, J.M., and Ingram, G.D. (1979). "Viscous attenuation of sound in saturated sand", J. Acoust. Soc. Am. 66, 1807-1812.

[4] Stoll, R.D., and Bryan, G. M. (1970). "Wave attenuation in saturated sediments", J. Acoust. Soc. Am. 47, 1440-1447.

[5] Stoll, R.D. (1977). "Acoustic waves in ocean sediments", Geophysics 42, 715-725.

[6] Zhubayev, A., and Ghose, R. (2012). "Contrasting behavior between dispersive seismic velocity and attenuation: Advantages in subsoil characterization", J. Acoust. Soc. Am. 131(2).